THE ASTROPHYSICAL JOURNAL, 427:134–139, 1994 May 20

MULTIPLE X-RAY EMISSION COMPONENTS IN LOW-POWER RADIO GALAXIES

D. M. WORRALL AND M. BIRKINSHAW
Harvard-Smithsonian Center for Astrophysics, 60 Garden Street, Cambridge, MA 02138
Received 1993 June 28; accepted 1993 November 19

ABSTRACT

We report X-ray observations of the first six sources observed with *ROSAT* in our study of low-power radio galaxies. Spatial and spectral measurements show that both resolved (thermal) and unresolved X-ray emission in a single source are typical, although the relative strength and size of the resolved component varies between objects. The unresolved X-ray component correlates well with the core radio emission and may be dominated by nonthermal emission associated with an inner radio jet.

Subject headings: galaxies: active — radio continuum: galaxies — radiation mechanisms: miscellaneous — X-rays: galaxies

1. INTRODUCTION

Although the *Einstein Observatory* found that low-power radio galaxies often emit X-rays (Feigelson & Berg 1983; Fabbiano et al. 1984), the dominant physical process responsible for the radiation has remained unclear. Studies of Cen A and M87 have indicated multiple X-ray components (Schreier et al. 1979; Feigelson et al. 1981; Schreier, Gorenstein, & Feigelson 1982; Biretta, Stern, & Harris 1991) including emission from the active nucleus, jet radiation most likely of synchrotron origin, and diffuse emission probably from hot gas which is now an established constituent of X-ray luminous elliptical galaxies (Forman, Jones, & Tucker 1985). The integrated thermal emission from the surrounding Virgo Cluster confuses the X-ray emission of M87 (Fabricant & Gorenstein 1983), and for some other low-power radio galaxies a thermal interpretation has been applied to all the X-ray emission (Morganti et al. 1988; Feretti et al. 1990) particularly where the source is resolved or there is known association with a cluster. Correlations have been found between the X-ray emission and both the core and extended radio emission. However, rather than clarifying the situation, these correlations have been used to argue both for a thermal origin (Feigelson & Berg 1983) and a nuclear origin (Fabbiano et al. 1984) for the X-ray emission in radio galaxies.

In this paper we show that a qualitative improvement in radio-galaxy X-ray research is afforded through *ROSAT* observations. Spatial and spectral measurements show that both resolved (thermal) and unresolved X-ray emission in a single source are typical. For different objects the relative strength of the emissions varies by an order of magnitude, and the linear extent of the gas by a larger factor. The unresolved X-ray component may be dominated by nonthermal emission associated with an inner radio jet.

2. X-RAY OBSERVATIONS AND ANALYSIS METHODS

We observed the radio galaxies listed in Table 1 in soft X-rays, at the center of the telescope field of view, with the *ROSAT* Position-Sensitive Proportional Counter (PSPC; Trümper 1983; Pfeffermann et al. 1987) during the pointed phase of the mission. They are the first sources observed as part of two ongoing programs; one studies a subsample of radio galaxies which Ulrich (1989) proposed are drawn from the parent population of BL Lac objects, and the other is a study of the emission in and around low-power radio galaxies with particularly prominent radio jets.

The data we received had already been corrected for instrumental effects and motion of the satellite. For further analysis we used the Post Reduction Off-line Software (PROS; Worrall et al. 1992) and additional software which we developed to convolve the energy-dependent PSPC point response function (PRF; Hasinger et al. 1992) with radially symmetric spatial models. Only counts within the energy band for which the PRF is well modeled (0.2–1.9 keV) are used in the analyses presented in this paper. Some of the data were filtered to remove times of high particle background, and, in some cases, regions around one or more faint contaminating sources were excluded from the analysis. We extracted a background-subtracted radial profile about the maximum-likelihood centroid of X-ray emission for each radio galaxy, and determined the spectral distribution of the counts in the profile. The radial profiles were typically extracted to a radius of 5′.7, with background from an annulus of radii 3′ to 5′.7 (see Fig. 1, where dotted curves mark the background annuli). The PSPC PRF ($\sim$25″ FWHM) is such that the analysis is sensitive to resolved components with radii in the range 3-60 kpc for the nearest galaxy, and 20–380 kpc for the most distant one. NGC 326 is the only source to show obvious asymmetric extended emission; the radial-profile analysis is presented here only to provide a qualitative comparison with the other sources. Its extension is largest toward the northeast; we have used only data between position angles 125° and 290° in order to characterize the minimum extent of the emission.

Best fits were determined for each radial profile to an unresolved component, a β model which is appropriate for gas in hydrostatic equilibrium (Cavaliere & Fusco-Femiano 1978; Sarazin 1986), and a combination of an unresolved component and a β model. Results in the tables are for $\beta = \frac{2}{3}$, which is close to values fitted for cluster gas (see, e.g., Sarazin 1986), whereas $\beta = \frac{1}{2}$ may be more typical for gas confined within nearby elliptical galaxies (Forman et al. 1985). Our choice is partly driven by the fact that $\beta \leq \frac{1}{2}$ gives an infinite X-ray flux so that an extra parameter (a cut-off radius) must be introduced into the models. In the present work we have not attempted to fit values of β from the slope of the power-law region of the model. Indeed, Figure 1 shows that only for the two least extended sources is there any possibility of doing this. Preliminary results give a preference for $\beta = \frac{1}{2}$ for NGC 4261 and $\beta = \frac{2}{3}$ for NGC 315. For the other four sources, the measured HWHM (half-width half-maximum) of the resolved

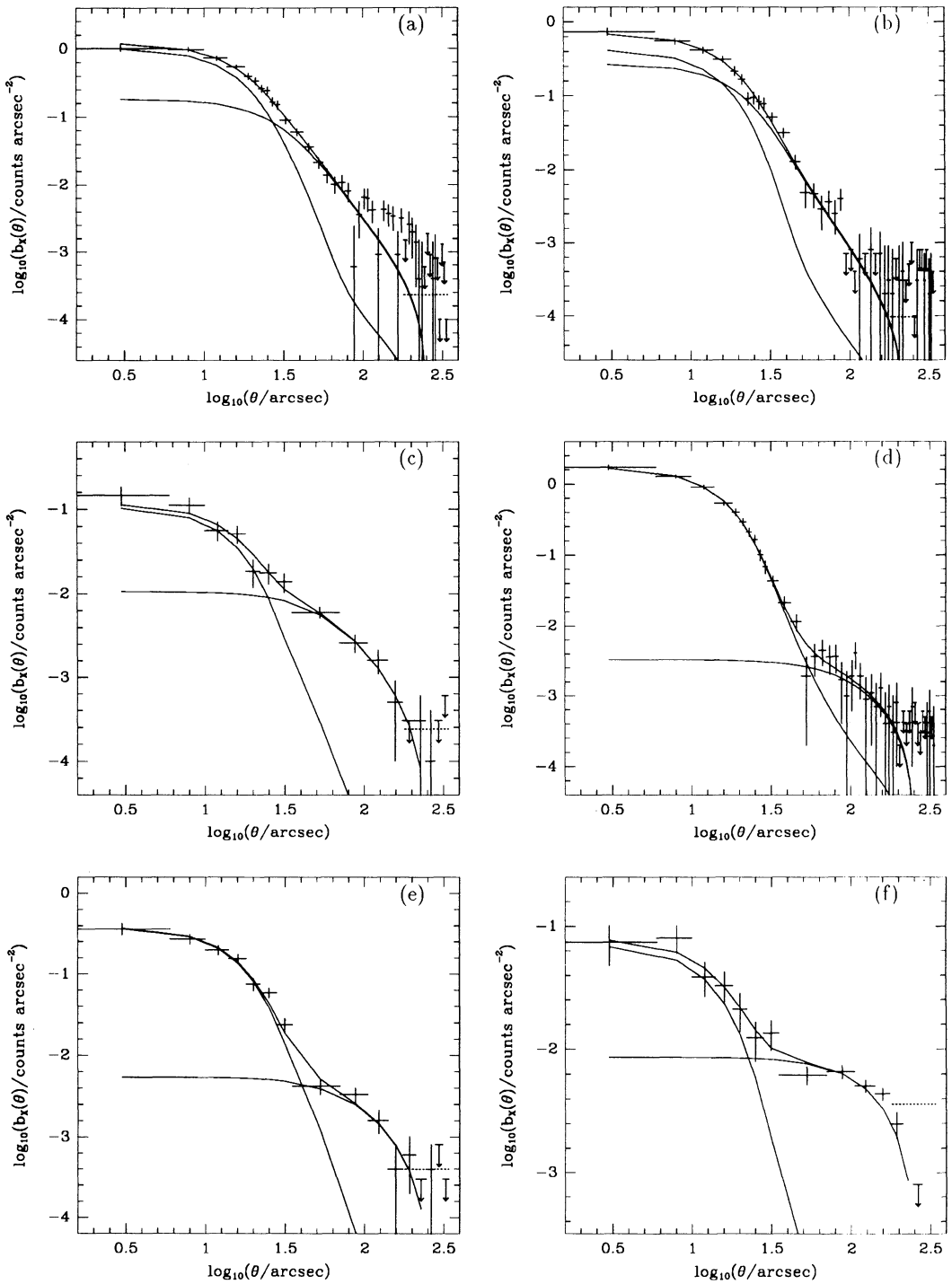

FIG. 1.—Background-subtracted X-ray radial profiles for radio galaxies in order of increasing intrinsic core-radius of the β model. (*a*) NGC 4261, (*b*) NGC 315, second exposure, (*c*) 4C 35.03, (*d*) NGC 6251, (*e*) NGC 2484, and (*f*) NGC 326. In all cases a combination of point source (*narrow curve*) and extended β model (*broad curve*) gives a better fit than either component alone (Table 2). The dotted curve shows the contribution, taken into account in the fitting, of the model to the background annulus.

X-ray emission is independent of the value assumed for β. Since

$$\mathrm{HWHM} \propto \theta_{cx}\sqrt{[2^{2/(6\beta-1)}-1]}\,,$$

we find $\theta_{cx}(\beta=\frac{1}{2}) = 0.77\theta_{cx}(\beta=\frac{2}{3})$; this factor can be applied to the values in Table 2 to calculate $\theta_{cx}(\beta=\frac{1}{2})$ for the most extended sources. For small X-ray extensions (NGC 4261 and NGC 315), a decreased β again suggests a smaller core radius, but the observations are sensitive only to the power-law wings of the β model and cannot constrain the core radius. The values in Table 2 should be treated as upper limits to θ_{cx} for NGC 4261 and NGC 315 for values of $\beta < \frac{2}{3}$

The counts in each background region contain a contribu-

TABLE 1

OBSERVATIONS

Object	Name B1950	z	Date	Exposure[a] (s)
NGC 315	0055+300	0.0165	1992 Jan 17–Feb 1	10,343
			1992 Jul 19–21	17,869
NGC 326	0055+265	0.047	1992 Jul 24–29	20,969
4C 35.03.....	0206+355	0.0375	1992 Jul 24–27	14,843
NGC 2484	0755+379	0.0413	1991 Oct 30–Nov 1	15,172
NGC 4261	1216+061	0.0073	1991 Dec 24–30	22,042
NGC 6251	1637+826	0.024	1991 Mar 13–16	14,830

[a] Time used in analysis. In some cases intervals of high background have been excluded.

tion from the outer part of the source emission. For all cases except NGC 326 (see § 6) the modeled source emission in the background annulus is $\leq 8\%$ of the counts in that annulus. This is small compared with the statistical errors in our radial profiles (see error bars in Fig. 1, and note that for the source with the smallest errors, NGC 4261, the contribution is 2%), and a correction for this emission is made in our model fitting. Each spatial model assumed an energy weighting which is the same as that in the total radial profile.

Our spectral fitting uses the latest versions of the PSPC response-matrix (no. 36) and effective-area (no. 2.6) calibrations. Best fits were determined for each observation to a power law, a thermal model (Raymond & Smith 1977) with 100% cosmic abundances, and a combination of the two.

Since *ROSAT* data currently have absolute positional uncertainties as large as 10″ over timescales of months (MPE 1992), and to provide an indication of systematic uncertainties in derived model-dependent quantities, we have analyzed separately the two observations of NGC 315 which were 6 months apart (Table 1).

A Friedmann cosmological model with $H_0 = 50$ km s^{-1} Mpc^{-1}, $q_0 = 0$, is used throughout this paper.

3. RESULTS OF SPATIAL ANALYSIS

The minimum χ^2 values for the three models fit to the radial profiles are given in Table 2. Only NGC 6251 fits unresolved emission acceptably. In all cases a better fit is obtained with an extended β model. However, the addition of an unresolved component to the β model gives a still smaller χ^2 and is greater than 99% significant, according to the F-test, for all sources except NGC 315, for which the β component is barely resolved (core radius $\theta_{cx} < 20''$) and component separation is difficult with the PSPC. Figure 1 shows the radial profiles and best-fit two-component models, and, like Table 2, is in order of increasing intrinsic core-radius, r_{cx}, of the β model.

TABLE 2

RADIAL-PROFILE MODEL FITS

Object	Unresolved Component χ^2/dof	β Model χ^2/dof	β Model θ''_{cx}	β + Unresolved χ^2/dof	β + Unresolved θ''_{cx}	r_{cx} kpc[a]
NGC 4261	436/45	79/44	7	54.4/43	21 ± 5	4
NGC 315[b]	117/45	56/44	4	51.3/43	17 ± 11	8
	164/45	46/44	5	43.4/43	9 ± 5	4
4C 35.03.....	325/16	36/15	25	8.2/14	70 ± 15	72
NGC 6251	52/45	43/44	1	25.3/43	130 ± 45	88
NGC 2484	118/16	35/15	3	12.5/14	110 ± 30	124
NGC 326[c]	2928/16	54/15	200	22.0/14	230 ± 30	294

NOTE.—In this table, $\beta = \frac{2}{3}$ assumed in all fits (see § 2).

[a] Fractional error same as in θ_{cx}. Errors are 1 σ.

[b] First and second exposures (Table 1) listed separately.

[c] X-ray emission very extended and not radially symmetric. Results for this source should be taken to be qualitative rather than quantitative.

To check that systematic errors in the aspect determination have a negligible effect on our results, we applied our analysis to two BL Lac objects and two quasars spanning similar exposure times and net counts to the radio galaxies; all fitted an unresolved component and excluded the presence of additional resolved X-ray emission of similar strength to that detected in the radio galaxies. The strongest constraint on systematic errors is provided by one of the quasars which has a longer exposure (24 ks) than any of the radio galaxies, and has net counts comparable to the median for the radio galaxies.

4. RESULTS OF SPECTRAL ANALYSIS

The same net counts which give the radial profiles of Figure 1 are used for our spectral fitting. The presence of a resolved X-ray component in or around each galaxy suggests that at least some of the emission is thermal. However, although the fits to a thermal spectrum are in most cases acceptable, in all cases the fit to a power law is better (Table 3). Since a power law is an unlikely model for extended emission of group or cluster dimension, a model which includes at least some thermal emission is suggested. We find similar, improved, and acceptable fits for either a combination of two temperatures or, as given in Table 3, a thermal plus a power law.

For the thermal plus power-law fit, the gas temperatures are similar for all sources except NGC 326, whose spectral parameters are subject to additional systematic uncertainty (see Table 3) and whose dominant resolved emission is of cluster dimension and quite plausibly hotter than 1 keV. When fit to two thermal components, most of the emission from NGC 326 is still from a hot gas of similar greater than 1 keV temperature, with the counts previously in a soft power law being fitted by very soft thermal emission. When the other sources are fitted to two thermal components, one is on average about 0.2 keV cooler than that given in Table 3; the other thermal component is generally more poorly constrained and of temperature greater than 1 keV.

None of the two-component spectral fits or single-temperature thermal fits requires absorption in excess of that from our Galaxy as determined using Stark et al. (1992). Only the unlikely single-component power law requires excess absorption to produce the spectral decrease which is measured in the lowest energy channels; such a decrease is an intrinsic feature of the low-temperature thermal components.

5. COMPOSITE RESULTS

Our spatial analysis found unresolved emission in all the galaxies, and additional resolved emission of galaxy dimension in the two nearest. To assess the possible contribution from the integrated emission of discrete X-ray sources similar to those in spiral galaxies, we have used the B_0^T magnitudes from de Vaucouleurs et al. (1991) and extrapolated 0.2–3.5 keV X-ray luminosities of components in our spectral fits for a comparison with the X-ray and optical luminosity correlation for spiral galaxies given in Figure 5 of Fabbiano, Gioia, & Trinchieri (1989). The X-ray luminosities of all the separate spectral components for the radio galaxies lie at least an order of magnitude above the corresponding X-ray luminosity in the spiral-galaxy

TABLE 3

SPECTRAL MODEL FITS

OBJECT	log $N_{H_{Gal}}$	NET COUNTS	POWER LAW χ^2/dof	THERMAL χ^2/dof	THERMAL + POWER LAW χ^2/dof	kT[a] (keV)	α[a]	log $N_{H_{int}}$[b]	L_{Th} 0.2–1.9 keV (W)	L_{PL}[c] 0.2–1.9 keV (W)
NGC 4261	20.20	1890 ± 106	26.3/21[d]	30.4/22	2.9/20	0.6 (+0.1, −0.1)	0.7 (+0.2, −0.2)	<20.6	1×10^{34}	1×10^{34}
NGC 315[e]	20.76	528 ± 51	14.5/21[d]	26.4/22	9.5/20	0.5 (+0.2, −0.2)	0.9 (+0.5, −0.9)	<21.7	4×10^{34}	7×10^{34}
	20.76	858 ± 66	13.2/21[d]	30.6/22	10.6/20	0.6 (+0.1, −0.2)	0.8 (+0.4, −0.6)	<22.0	4×10^{34}	6×10^{34}
4C 35.03	20.77	305 ± 54	6.9/22	7.1/22	5.7/20	0.8 (+0.8, −0.6)	−0.5 (+1.6, −1.5)	<22.4	6×10^{34}	9×10^{34}
NGC 6251[f]	20.74	1540 ± 78	10.3/21[d]	17.3/22	8.8/20	0.6 (+0.3, −0.3)[f]	0.4 (+0.2, −0.4)[f]	<21.9	8×10^{34}	3×10^{35}
NGC 2484	20.70	523 ± 67	5.1/21[d]	12.3/22	5.2/20	0.7 (+0.4, −0.5)	1.4 (+0.5, −0.7)	<21.8	8×10^{34}	4×10^{35}
NGC 326[g]	20.74	1401 ± 42[g]	51.6/22	146.0/22	20.0/20	3.0 (+1.6, −1.0)[g]	3.3 (+0.6, −0.4)[g]	<20.4	7×10^{35}	9×10^{35}

[a] Errors are 1 σ for one interesting parameter, allowing the other parameters to vary.
[b] 3 σ upper limits for one interesting parameter, allowing the other parameters to vary.
[c] Assuming isotropic emission over 4 π, but note that emission may be anisotropic.
[d] χ^2 reduces by more than unity for inclusion of intrinsic absorption. For the other fits this is not true and we include only Galactic absorption.
[e] First and second exposures (Table 1) listed separately.
[f] Consistent but better constrained spectral results for a broader *ROSAT* energy band are given by Birkinshaw & Worrall 1993.
[g] Net counts adjusted roughly for large model contribution in background region. An additional systematic uncertainty should be applied to the spectral parameters, which should not be used quantitatively (see § 6).

correlation and are comparable with or exceed 10^{34} W (the limiting X-ray luminosity of spiral galaxies). This argument applies to separate components in both the combined thermal fit and the thermal plus power-law fit, and it leaves hot gas as the most likely explanation for the bulk of the emission from any component which fits a thermal spectrum.

Although the X-ray data alone do not rule out a thermal origin for the entire X-ray emission that the PSPC measures, there is a reason for considering this unlikely. In the nearest two galaxies, all the emission under discussion (including the hotter, greater than 1 keV, component) is of galaxy dimension, and for NGC 6251 and NGC 2484 the hot spectral component must be related to the unresolved spatial component (within the galaxy) since these components dominate the counts in their respective analyses. Gas capable of producing this hot spectral component would be unlikely to be retained within the potential wells of these galaxies; the temperatures are more characteristic of the gas in a massive group of galaxies. NGC 6251 provides the largest number of counts and thus the best-constrained temperature for a hot component. In Birkinshaw & Worrall (1993), we have already presented these spectra in detail and argued that, even taking into account the companion galaxies to NGC 6251, there is no plausible site at which the hot component in a two-temperature fit to the data can be confined. From this and other self-consistency arguments we are led to prefer a power law plus thermal interpretation for the source. NGC 326 is different from the other galaxies presented here in that the resolved asymmetric emission is of cluster dimension, so that a smaller X-ray contribution from unresolved cooler gas is quite plausible.

Thermal plus power-law fits provide a natural interpretation that the power law is from the active core of the galaxy, and the less than 1 keV temperatures (Table 3) are very reasonable for gas associated with an elliptical galaxy or small group. To test this, Table 4 compares the fraction of counts in the unresolved component derived from the spatial fitting with the fraction of counts in the power law from the spectral fitting. The agreement is particularly good considering that the errors quoted are statistical only and do not include uncertainties in the model parameters, and the spatial analysis did not take into account the different spectral distributions of the β model and the unresolved component. The discrepancy is largest for NGC 326, but this is not surprising given the inadequacies of the current analysis for this obviously complex X-ray–emitting region. NGC 6251 is noteworthy as the only source where the spectral fitting gives significantly fewer counts in the power law than the spatial fitting gives in the unresolved emission. Birkinshaw & Worrall (1993) analyze the central emission in more detail and interpret the unresolved component as nonthermal emission mixed with a small amount of thermal emission from X-ray gas in a cooling flow (cf. § 7: a longer cooling time is found for the large-scale thermal component).

The remaining discussion will adopt the interpretation of the X-rays from these galaxies as unresolved emission with a predominantly power-law spectrum from the active core of the galaxy combined with resolved emission from a thermal gas. Meanwhile, we await approved observations of four of these galaxies with the *ROSAT* HRI to search for resolved components on spatial scales as small as $\sim 5''$ to test whether some fraction of the emission unresolved with the PSPC might not instead arise from thermal gas.

6. NOTES ON INDIVIDUAL SOURCES

Further results for individual sources will be presented in forthcoming papers. However, notes on two follow here.

NGC 4261.—The 3 σ upper limit for intrinsic N_H in the two-component (power-law plus thermal) spectral fit is

TABLE 4

PERCENTAGE OF COUNTS IN UNRESOLVED POWER LAW

Object	Spatial Fitting[a]	Spectral Fitting[a]
NGC 4261	51 ± 4	52 ± 6
NGC 315[b]	61 ± 7	57 ± 9
	41 ± 5	54 ± 7
4C 35.03	29 ± 6	52 ± 15
NGC 6251	93 ± 5	78 ± 6
NGC 2484	65 ± 9	76 ± 15
NGC 326	10 ± 2	25 ± 2

[a] 1 σ statistical errors for best-fit model. Errors due to uncertainties in the model parameters are not included.
[b] First and second exposures (Table 1) listed separately.

4×10^{20} atoms cm^{-2}. This is ~ 10 times smaller than the value inferred from CO absorption (Jaffe & McNamara 1994) against the millimeter-emission from the nuclear radio source. Such a large difference between the H_2 absorbing column and the inferred X-ray absorbing column is unexpected and requires explanation. If a large fraction of the unresolved X-ray emission from NGC 4261 originates from the same region in the nucleus that produces the millimeter-wave emission, then one possibility is that the mean X-ray and millimeter-wave lines of sight to that emission differ. This could arise because of extreme clumping in the molecular material if the detailed X-ray and millimeter-wave structures of the nucleus are different. Alternatively, the X-rays could emerge from the nucleus along a hole in a dense molecular torus, and be scattered toward the observer by circumnuclear plasma, while the millimeter-wave radiation takes a direct path through the torus: such a model has been used for NGC 1068 (Elvis & Lawrence 1988). Another possibility is that the excitation temperature of the molecular gas and the CO/H_2 abundance might be substantially different from those in our Galaxy, so that the H_2 column has been overestimated. Finally, it is possible that the X-ray spectrum of NGC 4261 contains a strong soft component that is absorbed in our data by the H_2 column implied by the CO absorption—but then the strength of that soft component and the column density in H_2 are required to be in coincidental balance. Further work on the X-ray and radio data are needed to make progress in testing these possibilities: optical spectropolarimetry of the nucleus of the galaxy would also be helpful.

NGC 326.—Obvious large-scale asymmetric X-ray emission is found. The results presented here for this source are qualitative only, since radial symmetry is not an adequate spatial representation, and the spectral and spatial analyses incorporated only approximate adjustments for the large model contribution in the background region (see § 2). In view of this structure (to be discussed elsewhere) the errors in Table 3 are likely to be grossly underestimated.

7. THE THERMAL COMPONENT

Table 5 gives the mean cooling time for gas within r_{cx}, using equations (10) and (25) of Birkinshaw & Worrall (1993) and the spatial and spectral parameters derived from our two-component (power-law plus thermal) fits. Only for NGC 4261 and NGC 315, where the hot gas is of galaxy rather than cluster dimensions (see Table 2), is the cooling time short enough that a cooling flow may have begun. For NGC 6251 we have argued elsewhere (Birkinshaw & Worrall 1993, and see § 5) that the spectral results support a small thermal contribution to the unresolved emission and that this gas, which is in a cooling flow, provides infalling energy which can power the active nucleus. It remains possible for the other sources that some or all of the unresolved emission is thermal and in a cooling flow, and forthcoming *ROSAT* HRI observations will test this possibility through improved spatial resolution (see discussion in § 5).

TABLE 5

GAS COOLING TIME

Object	t_{cool} within Core Radius (yr)[a]
NGC 4261	3.4×10^9
NGC 315[b]	4.0×10^9
	1.4×10^9
4C 35.03	5.2×10^{10}
NGC 6251	1.0×10^{11}
NGC 2484	9.8×10^{10}
NGC 326	1.2×10^{11}

[a] Uncertainties indicated by the difference between the two results for NGC 315. Weak dependence on Hubble constant; $t_{cool} \propto H_0^{-1/2}$. Value should be compared with the Hubble time, which is $\sim 2 \times 10^{10} (H_0/50$ km s^{-1} Mpc$^{-1})^{-1}$ yr for $q_0 = 0$. Less than $\sim 25\%$ decrease in t_{cool} if $\beta = \frac{1}{2}$ (rather than $\beta = \frac{2}{3}$ assumed here).

[b] First and second exposures (Table 1) listed separately.

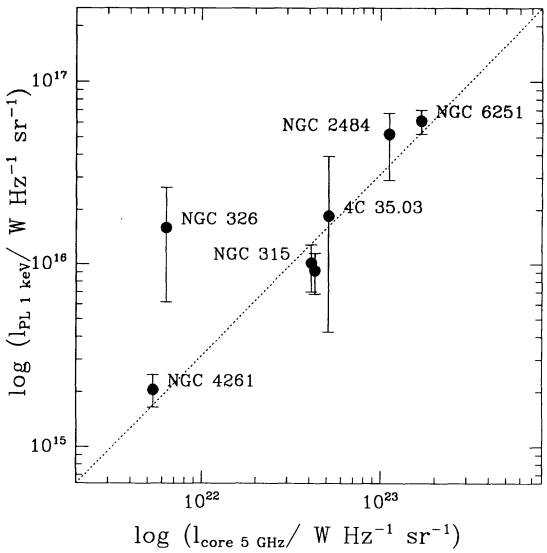

FIG. 2.—1 keV X-ray spectral luminosity for the power-law component in the two-component spectral fit plotted against 5 GHz radio-core spectral luminosity (see Table 6). The X-ray errors are 1 σ for one interesting parameter, allowing the other parameters to vary. An additional large systematic error should be applied to the derived X-ray value for NGC 326 since the source is dominated by nonradially symmetric extended emission (see § 2) and the unresolved component may contain substantial thermal emission (see § 5). The dotted line is of slope unity.

8. THE NONTHERMAL COMPONENT

Support for the nonthermal nature of most of the unresolved X-ray emission is shown in Figure 2 where the X-ray spectral luminosity of this component (from our spectral analysis) is plotted against the spectral luminosity of the radio core (see Table 6). Although NGC 326 is shown, its X-ray spectral luminosity is highly uncertain and is likely to be overestimated (see caption). The other sources shown are consistent with pro-

TABLE 6

NONTHERMAL EMISSION

Object	S_{PL} (1 keV) (nJy)	S_{core} (5 GHz) (mJy)	S_{Tot}[a] (5 GHz) (mJy)	Radio References
NGC 4261	112 (+23, −22)	293	4200	1, 2, 3
NGC 315[b]	107 (+28, −33)	450	1050	2, 3, 4
	97 (+24, −25)	...	...	...
4C 35.03	39 (+44, −30)	106	1000	2, 3, 5
NGC 6251	308 (+44, −47)	850	1550	6
NGC 2484	84 (+25, −37)	190	1050	2, 3, 5
NGC 326	18 (+12, −11)	8.6	600	2, 3, 7

[a] $\sim 15\%$ uncertainty.

[b] First and second exposures (Table 1) listed separately.

REFERENCES.—(1) Birkinshaw & Davies 1993; (2) Becker, White & Edwards 1991; (3) Gregory & Condon 1991; (4) Venturi et al. 1993; (5) Giovannini, Feretti, & Comoretto 1990; (6) Jones et al. 1986; (7) Fomalont 1993 (private communication).

portionality between the X-ray and radio emission, in support of a model where the X-rays originate as nonthermal emission from the inner regions of a parsec-scale radio jet.

The X-ray (power-law) spectral indices (Table 3) are not well constrained, but are generally consistent with values for BL Lac objects (Worrall & Wilkes 1990), the sources proposed as low-power radio galaxies with relativistic radio jets in the line of sight of the observer (e.g., Wardle, Moore, & Angel 1984). Our results are in qualitative agreement with such a "unified" model.

9. CONCLUSIONS

The *ROSAT* spectral and spatial results are self-consistent in indicating that low-power radio galaxies emit at least two components of X-rays. One component is resolved. It can be modeled spatially with a β model, and a thermal origin is also supported by spectral fitting. The hot gas is of a dimension ranging from galaxy size (for NGC 4261 and NGC 315) to cluster size (for NGC 326). Only the gas of galaxy scale cools fast enough that a cooling flow may have begun.

The second X-ray component is unresolved. It is likely to be predominantly thermal in NGC 326, which differs from the other sources in that the resolved emission is relatively stronger, larger, and nonradially symmetric. For the other sources, a proportionality between the unresolved X-ray and core radio emission supports the dominant origin for the unresolved X-ray emission as nonthermal radiation from the inner regions of a parsec-scale radio jet. A nonthermal origin for most of the unresolved emission in NGC 6251 has already been argued on the basis of more detailed work by Birkinshaw & Worrall (1993).

The sources studied show an order of magnitude range in the relative strength of the unresolved and resolved emission, and, since we are measuring components only on angular sizes between 15″ and 5′, the linear sizes of emission which can be resolved is influenced by the galaxy redshifts. In the closest radio galaxies, NGC 4261 and NGC 315, low-level thermal emission of group or cluster dimension becomes hard to measure because of its relatively large angular size. Evidence for such emission around NGC 4261 has been found by Davis et al. (1994), perhaps explaining the small apparent excess over our model profile at radii 2′–4′ (Fig. 1*a*). Conversely, gas of galaxy dimension in the other sources would lie within the PRF of the PSPC; however, an argument limiting this to a small fraction of the core X-radiation in NGC 6251 has been presented by Birkinshaw & Worrall (1993) based on detailed X-ray spectral analysis.

ROSAT has provided a major advance in radio-galaxy X-ray research by showing that a mixture of resolved (thermal) and unresolved emission is typical. This situation appears to apply also to high-power radio galaxies; Worrall et al. (1994) report similar findings in the $z = 1$, high-power, radio galaxy 3C 280.

The measurement of multiple X-ray emission components has implications for models in which BL Lac objects are low-power radio galaxies with their parsec-scale relativistic jets in the line of sight. Padovani & Urry (1990) used *Einstein Observatory* data to construct X-ray luminosity functions for BL Lac objects and radio galaxies assuming that the intrinsic luminosity of the jet is some fixed fraction of an unbeamed luminosity. Birkinshaw & Worrall (1993) argued on the basis of results for NGC 6251 that thermal X-ray emission may be the source of the required unbeamed X-ray emission. However, the current work would not appear to support this suggestion. Table 3 shows that in every case the power-law luminosity (assuming that the X-rays are radiated isotropically) exceeds the thermal luminosity. Thus, by Padovani & Urry's definition every object would be classed as a BL Lac object rather than a radio galaxy, in violation of the selection of objects used to construct the luminosity functions. Consistency would appear to require part of the measured unresolved X-ray emission to be unbeamed, perhaps through a contribution from unresolved hot gas or because of a velocity or collimation gradient in an X-ray–emitting jet (Ghisellini & Maraschi 1989; Maraschi, Celotti & Ghisellini 1992). Further discussion and more detailed results for individual sources will be presented elsewhere.

We thank Walter Jaffe and Brian McNamara for transmitting prepublication results on the neutral gas in NGC 4261, and Martin Elvis and the referee for comments which improved the paper. Our work was funded by NASA grants NAG 5-1882 and NAG 5-2312, and NASA contract NAS 8-39073.

REFERENCES

Becker, R. L., White, R. L., & Edwards, A. L. 1991, ApJS, 75, 1
Biretta, J. A., Stern, C. P., & Harris, D. E. 1991, AJ, 101, 1632
Birkinshaw, M., & Davies, R. D. 1994, in preparation
Birkinshaw, M., & Worrall, D. M. 1993, ApJ, 412, 568
Cavaliere, A., & Fusco-Femiano, R. 1978, A&A, 70, 677
Davis, D. S., et al. 1994, in preparation
de Vaucouleurs, G., de Vaucouleurs, A., Corwin, H. G., Buta, R. J., Paturel, G., & Fouqué, P. 1991, Third Reference Catalogue of Bright Galaxies (Berlin: Springer-Verlag)
Elvis, M., & Lawrence, A. 1988, ApJ, 333, 161
Fabbiano, G., Gioia, I. M., & Trinchieri, G. 1989, ApJ, 347, 127
Fabbiano, G., Miller, L., Trinchieri, G., Longair, M., & Elvis, M. 1984, ApJ, 277, 115
Fabricant, D., & Gorenstein, P. 1983, ApJ, 267, 535
Feigelson, E. D., Schreier, E. J., Delvaille, J. P., Giacconi, R., Grindlay, J. E., & Lightman, A. P. 1981, ApJ, 251, 31
Feigelson, E. D., & Berg, C. J. 1983, ApJ, 269, 400
Feretti, L., Spazzoli, O., Gioia, I. M., Giovannini, G., & Gregorini, L. 1990, A&A, 233, 325
Forman, W., Jones, C., & Tucker, W. 1985, ApJ, 293, 102
Ghisellini, G., & Maraschi, L. 1989, ApJ, 340, 181
Giovannini, G., Feretti, L., & Comoretto, G. 1990, ApJ, 358, 159
Gregory, P. C., & Condon, J. J. 1991, ApJS, 75, 1011
Hasinger, G., Turner, T. J., George, I. M., & Boese, G. 1992, NASA/GSFC/OGIP, Calibration Memo CAL/ROS/92-001
Jaffe, W., & McNamara, B. R. 1994, submitted to ApJ
Jones, D. L., et al. 1986, ApJ, 305, 684
Maraschi, L., Celotti, A., & Ghisellini, G. 1992, in Physics of Active Nuclei, ed. W. J. Duschl & S. J. Wagner (Berlin: Springer-Verlag), 605
Max Planck Institut für Extraterrestrische Physik (MPE) 1992, *ROSAT* Newsletter No. 10
Morganti, R., Fanti, R., Gioia, I. M., Harris, D. E., Parma, P., & de Ruiter, H. 1988, A&A, 189, 11
Padovani, P., & Urry, C. M. 1990, ApJ, 356, 75
Pfeffermann, E., et al. 1987, in Soft X-ray Optics & Technology, ed. E.-E. Koch & G. Schmahl (Proc. SPIE 733), 519
Raymond, J. C., & Smith, B. W. 1977, ApJS, 35, 419
Sarazin, C. L. 1986, Rev. Mod. Phys., 58, 1
Schreier, E. J., Feigelson, E., Delvaille, J., Giacconi, R., Grindlay, J., Schwartz, D. A., & Fabian, A. C. 1979, ApJ, 234, L39
Schreir, E. J., Gorenstein, P., & Feigelson, E. D. 1982, ApJ, 261, 42
Stark, A. A., Gammie, C. F., Wilson, R. W., Bally, J., Linke, R. A., Heiles, C., & Hurwitz, M. 1992, ApJS, 79, 77
Trümper, J. 1983, Adv. Space. Res., 2, 241
Ulrich, M.-H. 1989, in BL Lac Objects, ed. L. Maraschi, T., Maccacaro., & M.-H. Ulrich (Berlin: Springer-Verlag), 45
Venturi, T., Feretti, L., Giovannini, G., Comoretto, G., & Wehrle, A. E. 1993, ApJ, 408, 81
Wardle, J. F. C., Moore, R. L., & Angel, J. R. P. 1984, ApJ, 279, 93
Worrall, D. M., & Wilkes, B. J. 1990, ApJ, 360, 396
Worrall, D. M., et al. 1992, in Data Analysis in Astronomy IV, ed. V. Di Gesu et al. (New York: Plenum), 145
Worrall, D. M., Lawrence, C. R., Pearson, T. J., & Readhead, A. C. S. 1994, ApJ (Letters), in press